IUST
Iran University of Science and Technology

Iranian Journal of Electrical and Electronic Engineering

Journal Homepage: ijeee.iust.ac.ir

Enhancing Network Efficiency through Dynamic Reconfiguration with Consideration of Renewable Energy Distributed Generation in Real-Time Operation

Ola. Badran*(C.A.)

Abstract: Dynamic Network Reconfiguration (DNR) is a vital and effective technique for reducing energy loss. Due to its complexity, nonlinearity, and large-scale optimization challenge, DNR is still a very difficult problem. This paper presents a new strategy for improving the DNR's stability and reliability under Real-Time Operation Mode (RTOM). It addresses a simultaneous optimization technique within various limitations and constraints about network power flow, voltage limits, output generation of Renewable Energy Resources (RER), Distributed generation mode, and network load profile. In real-time operating mode, it optimizes Distributed Generations Sizing and Location (DG_SL) for Renewable Energy and Dynamic Network Reconfiguration (DNR). Reducing the overall daily active and reactive energy losses of the network, raising the Voltage Stability Index (VSI), distributing the load more evenly, and enhancing distribution efficiency in real-time operation mode are the primary goals. A Multi-Objective Decision-Making Approach (MODMA) based on the Analytic-Hierarchy Process (AHP) and Crow Search Algorithm (CSA). To evaluate the practicality of the proposed method, MATLAB simulations were conducted on the IEEE 33- and 69-bus networks. In the IEEE 33-bus case, the proposed AHP–CSA framework achieves up to 91.75% reduction in daily active losses and more than 90.70% reduction in daily reactive losses, with the Voltage Stability Index consistently improved toward unity. In the IEEE 69-bus case, the method delivers up to 81.78% reduction in daily active losses and 59.78% reduction in daily reactive losses, also enhancing the overall voltage stability profile. These outcomes confirm the effectiveness and robustness of the proposed approach for real-time distribution network operation with renewable DG integration.

Keywords: Dynamic Network Reconfiguration, Multi-Objective Decision-Making Approach, distributed generation, power loss, Voltage Stability index, optimization technique.

1 Introduction

SINCE electricity is the foundation of all technologies, it is essential to humankind. A power system that consists of generating, distribution, and transmission produces electricity. The distribution area's flowing current results in power loss (Pl) [1]. Research [2, 3] has indicated that the distribution system (DS) experiences a higher loss than the transmission system. Therefore, one of the most important problems for distribution organizations is a power outage in the network [4]. To make up for these losses, more power is needed; nonetheless, doing so could result in income loss and long-term environmental issues[5, 6]. Thus, since reducing Pl enhances power quality and system efficiency, the majority of works anticipate reducing losses through the DS [7, 8]. Pl is decreased by installing locally distributed generation (DG). A distributed

Iranian Journal of Electrical & Electronic Engineering, 2026.
Paper first received 04 Sep 2024 and accepted 24 Nov 2025.
* The author is with the Department of Electrical Engineering-Industrial Automation, Faculty of Engineering and Technology, Palestine Technical University – Kadoorie, Tulkarm, Palestine.
E-mail: o.badran@ptuk.edu.ps.
Corresponding Author: Ola. Badran.

generation is a small generating unit located at a strategic place within the DS. These units, which would lower total pollution are usually RER and include mini-hydro, wind, photovoltaics, and biofuel [9].

Several methods have recently been employed to improve the quality of the modern system. DG_SL, or Distributed Generations Sizing and Location, is one such method. The best active power generation from the DG power generator unit is known as DG sizing, and the best placement of the generation units within the DS is known as DG location; these units are typically found close to the demand [10-12]. As demonstrated in [13, 14], the voltage system was enhanced and overall losses were decreased using the DG_SL approach. Thus, the optimal output and sit of DGs within the system are critical and vital to ensuring the power system operates effectively. In [15, 16], a photovoltaic (PV) system was presented with storage units to power a standalone system.

The most popular method for altering a modern network's performance, such as improving voltage quality, lowering Pl, and balancing the load, is network reconfiguration (NR) [17]. During the reconfiguration process, the distribution switches' statuses are changed by closing and opening the sectionalizing and tie switches, all the while preserving the network's radiality, the loads' feed connections, and the system voltage within permitted bounds [18]. The Distribution Reconfiguration (DR) method is critical and essential since it is a large-scale and nonlinear optimization problem that is also subject to some constraints and limitations [19]. As a result, numerous efforts aim to create effective solutions to address this problem [20]. The goals of the DR process are to balance the system load, improve voltage, decrease loss, isolate the fault area, and increase system stability and reliability [21-24].

The best method for improving the functionality of the current network operating system is to integrate DG into the system [25, 26]. A review of the simultaneous DR problem with DG to manage loss and voltage volatility was presented in [27]. The authors of [28] discussed multi-objective techniques for incorporating DG into the DR to lower Pl, operating costs, and pollutant gas emissions. An MPSO technique was applied in [29] to raise system voltage and lower loss. This methodology improved its efficiency in identifying the optimal output by utilizing both the binary and standard PSOs. A hybrid GWO and PSO approach to address the DR problem with both conventional and renewable DG units was suggested in [30]. Outcomes from the hybrid optimizer were superior to those from the individual one. The study in [31] introduced a novel approach to DR, DG_SL, and protection device challenges that make use of FA and EP. This seeks to spare the protective devices' protection during faults and normal cases of the system operation. To increase network reliability and lower Pl expenses, the researchers proposed a simultaneous optimal DR with ideal wind turbine and solar panel sites in [32, 33]. A novel method for figuring out the best switching sequence (SS) to use to alter the network's initial configuration to the optimal configuration was put forth in [34]. The objective of this method is to lower the loss and improve the Voltage Profile (VF) in real-time operation.

Furthermore, because Pl varies immediately with load, assessing network performance under dynamic loads is particularly crucial. A novel method for utilizing both static and dynamic loads to calculate the ideal SS for various test systems was presented in [35]. The goal of the study was to raise the VF and reduce the daily Pl. PV, mini-hydro, and biomass generators were incorporated into the DS [36] to alter the network's performance under dynamic load. To maximize system operation in a coordinated fashion, the work in [37] proposes an improved model that accounts for the unpredictable nature of distributed RER, DNR, and energy storage systems. The project seeks to promote the decarbonization of the electrical system and the deployment of DRES. In [38], an analysis of the hourly reconfiguration's value in the presence of RER was presented. A mathematical model is created to achieve this, applying hourly reconfigurations to lower daily network losses.

In contrast to prior studies such as [39] and [40], which focused on either reconfiguration alone or learning-based control, the present work introduces a hybrid MODMA approach based on AHP and CSA that simultaneously optimizes DNR and DG_SL under real-time operational constraints. This integration allows significant reductions in both active and reactive daily energy losses, while improving VSI and overall distribution network reliability.

2 Problem Formulation

In this section, the proposed methodology is adapted to determine the network configuration that is suitable for 24 hours integrated with DG sizing and location units. The major aim is to get the min active and reactive total daily energy loss, the best VSI, improve the network efficiency and balance the loads that enhance the system's stability and reliability during 24 hours. That is done under different technical constraints and limitations related to network power flow, voltage limits, renewable energy resources output generation, distributed generations mode, and network load profile.

All objective variables, including active and reactive power losses as well as the Voltage Stability Index (VSI), were expressed in per unit (p.u.) form prior to their integration into the fitness function. This normalization ensured that the terms of the fitness function remained dimensionless and directly

comparable, thereby allowing consistent weighting and balanced optimization results.

The problem can be formulated based on the MODMA approach using the following equations:

$$\text{Minimize\_F} = \sum_{hr}^{T}(w_1\ \text{Ploss} + w_2\ \text{Qloss} + w_3\ \text{SI}) \quad (1)$$

where w_1, w_2, and w_3 are the weight factors of the fitness (F). The terms of the fitness must be unitless, as follows:

$$\text{Ploss} = \frac{P_{loss}^{R}}{P_{loss}^{0}} \quad (2)$$

$$P_{loss} = \sum_{N=1}^{M}(R_N \times |I_N|^2) \quad (3)$$

where Ploss is the real Pl, P_{loss}^{R} is the real Pl after DDR, P_{loss}^{0} is the real Pl before DDR, R_N is the branch N resistance, I_N is the current through branch N.

$$\text{Qloss} = \frac{Q_{loss}^{R}}{Q_{loss}^{0}} \quad (4)$$

$$Q_{loss} = \sum_{N=1}^{M}(X_N \times |I_N|^2) \quad (5)$$

where Qloss is the imaginary Pl, Q_{loss}^{R} is the imaginary Pl after DDR, Q_{loss}^{0} is the imaginary power before DDR, and X_N is the branch N reactance.

The Voltage Stability Index (VSI) is examined to be maximized. That is looked to find the weakest bus voltage in the network which causes VS problems when load variation. VSI is widely accepted for radial distribution networks, computationally efficient for iterative optimization, and provides a clear and interpretable stability margin ranging between 0 and 1. These features make it highly suitable for real-time reconfiguration studies with DG integration. The expression of the VSI Index is as follows [41]:

$$\text{VSI} = |V_s|^4 - 4 \times \{P_r X_{ij} - Q_r r_{ij}\}^2 - 4 \times \{P_r r_{ij} - Q_r X_{ij}\}^2 \times |V_s|^2 \geq 0 \quad (6)$$

where V_s is the sending bus voltage in pu, P_r and Q_r are the power load in the active and reactive form at the bus receiving end in pu, respectively, r_{ij} and X_{ij} are the resistance and reactance of the line $i-j$ in pu, respectively.

During the stability operation of the system, the value of the VSI index must be greater than zero for each bus. That means buses become more stable when the value of the VSI index becomes closer to one for all buses. Thus, the bus having the lowest value of VSI (the weakest bus) will be considered in the fitness function. To integrate the VSI index into the fitness function, the modified index (SI) is taken as follows:

$$\text{SI} = \frac{1-\min(\text{VSI})}{\max(\text{VSI})} \quad (7)$$

where $\max(\text{VSI})$ and $\min(\text{VSI})$ are the buses that have the highest and lowest values of VSI, respectively. In this case, the SI term of fitness function also becomes unit less. Now the fitness function is harmonious and easily minimizes the Ploss and Qloss, and improves the VSI to enhance the system's stability and reliability.

The proposed method which represents the DDR and DG_SL must fulfill these limitations and constraints, as follows:

1. Power Constraints

The first one is the power injection constraint, which prevents the power flow from the DG units to the main grid since it causes protection problems, as shown in the following formulas [31].

$$\sum_{i=1}^{k} P_{DG,i} < \sum_{n}^{nbus}\left(P_{Load_n}\right) + P_{loss} \quad (8)$$

where $P_{DG,i}$ is the active power of the DG, k is the DG number, and nbus is the bus number.

The second one is the power balance constraint. This constraint achieves the equilibrium principle. Which means the power demand must be equal to the power supply. In other meaning, the active power supplied must equal the sum of the Ploss and active power load. In addition, the reactive power supplied must equal the sum of the Qloss and reactive power load as shown by the following equations [31]:

$$\sum_{i=1}^{k} P_{DG,i} + P_{Sub} = P_{Load} + P_{loss} \quad (9)$$

where P_{Load_n} is the active power of the load, respectively, and P_{Sub} is the active power of the main substation, respectively.

2. DG Constraints

$$P_i^{min} \leq P_{DG,i} \leq P_i^{max} \quad (10)$$

where P_i^{max} and P_i^{min} are the suitable limits of the DG.

3. Voltage Limits

$$V_{min} \leq V_{bus} \leq V_{max} \quad (11)$$

where V_{bus} is the bus voltage, and V_{min} and V_{max} are the bus's acceptable max and min voltage limits, respectively. The acceptable limitations between 0.95 p.u and 1.05 p.u (±5% of rated value) [42].

4. Network Topology Constraint

One of the most essential constraints is the topology constraint which aims to make the network in a radial form. The radial form is characterized by its simplicity in design and maintenance which in turn reduces the cost of operational and construction costs [43, 44]. To ensure radiality after the CSA optimization, each candidate configuration is validated through the branch–bus incidence matrix. Solutions forming loops or parallel feeder paths are penalized and excluded, allowing only feasible radial structures to remain in the optimization process.

5. Load Constraint

All branches must be supplied from the grid.

3 Proposed Approach

This section presents a novel method for simultaneously determining the optimal DNR integrated with the optimal DG_SL units during real-time operation mode. To ascertain the multi-objective function weight

factors, the AHP method is employed. The CSA technique is employed to determine the optimal DNR configuration and DG's-SL for 24 hours. The strategy is to increase VSI, balance loads, improve system efficiency, and decrease active and reactive total daily energy losses to enhance the DDN system's stability and reliability.

3.1 Analytic-Hierarchy Process (AHP)

AHP is applied as a decision-making tool to calculate the weight factors of multiple operating indices. It provides a systematic way to handle several criteria simultaneously, and the resulting relative relevance matrix is presented in Table 1.

Table 1. Relative importance matrix.

Definition Importance	Number Rate	Decimal Reciprocal
Equal	1	1
Moderate	3	0.3333
Strong	5	0.2000
Very strong	7	0.1429
Extreme	9	0.1111

Table 1. The weight factors estimation is presented in Table 2 based on the matrix scale arrangement. Where the total values were obtained by summing each row, and the weights were subsequently calculated as the ratio of each total to the overall sum. Fig. 1 presents the AHP approach steps.

Table 2. Weights from the AHP approach.

Criteria	Ploss	Qloss	VSI	Total	Weight
Ploss	1	5	7	13	0.7447
Qloss	0.2	1	1.4	2.6	0.1489
VSI	0.1429	0.7143	1	1.8572	0.1064
Sum				17.4572	1

3.2 Crow Search Algorithm (CSA)

The crow search algorithm is a population-based metaheuristic that draws inspiration from nature. Technique addressed by A. Askarazadeh in 2016 [45]. That imitates the social interactions and clever behaviors of the crow. Crows dwell in groups or flocks and hide their food in various locations. When necessary, even after several months, these perceptive crows can collect the hidden food since they have memorized the hiding spots. It is known that crows steal each other and purloin the other birds' food once they leave. Then crows can find the safest way to save their food from thieves and avoid being victims in the future. Crows are sentient birds that can recognize faces and coordinate their movements in anticipation of an intruding visitor [46, 47].

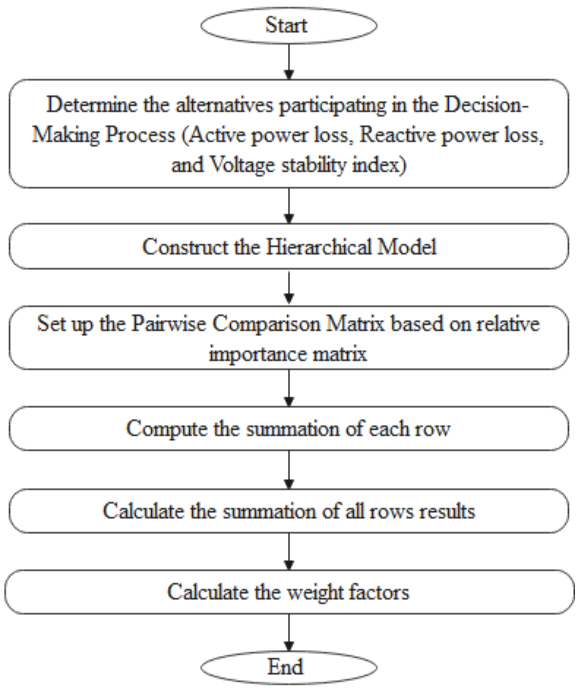

Fig. 1 AHP approach flowchart.

The CSA technique principle is as follows [48]:

1. Crows are a flock animal.
2. Crows can learn where they hide food.
3. Crows engage in purloining, following one another.
4. Crows guard their secret stockpiles against theft.

The implementation steps of the proposed methodology (simultaneous DNR and DG_SL during real-time operation mode) using CSA are as follows:

Step 1: Initialize the optimization problem and determine the CSA alterable parameters
Determine the optimization problem, the decision variable, and the limitations and constraints. Set the population number of crows (flock size = N), the max iterations number (tmax), the awareness probability (AP), and the flight length (fl).

Step 2: Set the DN parameters such as lines' resistance and reactance values, the initial values of the buses' voltages, bus load, PV generation output, DG mode, and load profile.

Step 3: Insert the weight factors calculated from the AHP approach into the fitness function formula.

Step 4: Initialize the crows' position
Assume X_i^t presents the position of each crow i in tth iteration as follows:

$$X_i^t = SW_{i,1}^t, SW_{i,2}^t, \dots, SW_{i,n}^t, DG\_L_{i,1}^t, DG\_L_{i,2}^t, \dots, DG\_L_{i,q}^t, DG\_S_{i,1}^t, DG\_S_{i,2}^t, \dots, DG\_S_{i,q}^t \quad (12)$$

where SW is the tie switch, DG is the distributed generation, (i = 1, 2, …, N), (t = 1, 2, …, tmax), n is the dimension of switch, q is the dimension of DG, DG_L is the location of DG, DG_S is the size of DG. Each crow X_i^t are randomly located in a d-dimensional search space and present a possible solution to the optimization problem.

Step 5: Initialize the crows' memory
Let m_i^t presents the memory of each crow i in tth iteration as follows:

$$m_i^t = m_{SW_{i,1}}^t, m_{SW_{i,2}}^t, \dots, m_{SW_{i,n}}^t, m\_DG\_L_{i,1}^t, m\_DG\_L_{i,2}^t, \dots, m\_DG\_L_{i,q}^t, m\_DG\_S_{i,1}^t, m\_DG\_S_{i,2}^t, \dots, m\_DG\_S_{i,q}^t \quad (13)$$

Step 6: Evaluate the value of the fitness
Use the load flow code based on the Newton–Raphson methodology to calculate the value of Ploss and Qloss, and Max and Min values of the distribution buses' voltages. Then evaluate the fitness using equation (1) for each crow in the matrix (15). Thus, the fitness value was calculated for one day (24 hr.).

Step 7: Update new position
Suppose crow i wants to update its position. Crow i follows crow j for example (any one of the flock crows) without knowing crow j and as a result crow i discovers the hidden position of the crow j foods. Thus, the position of crow i is updated based on the following expression:

$$X_i^{t+1} = X_i^t + (r_i * fl_i^t * (m_j^t - X)) \quad (14)$$

where X_i^{t+1} is the new or the updated position of crow i at $(t + 1)$ th iteration, r is a random value with a uniform distribution between 0 and 1, and fl_i^t is flight length at $(t + 1)$ th iteration. Now if crow i follows crow j and crow j observe that crow i follows it. Thus, crow j tries to fool crow i by moving randomly. This way can be presented based on the following formula:

$$X_i^{t+1} = \begin{cases} X_i^t + \left(r_i * fl_i^t * \left(m_j^t - X_i^t\right)\right) & \text{if } r_j \geq AP_j^t \\ \text{A random position} & \text{Otherwise} \end{cases} \quad (15)$$

where AP_j^t is the awareness probability of crow j at tth iteration. This process (step 7) is repeated for all crows.

Step 8: Check the feasibility of updating (new) positions
All new positions for all crows are checked to verify that it is under all limitations and constraints of the optimization process. Update the crow position if the new position of the crow is feasible. If the new position exceeds any of the limitations or constraints, the failed position changes with a feasible one from the initial position.

Step 9: Evaluate the fitness of the updated positions (new)
Calculate the fitness for each crow's new position for one day (24 hr.).

Step 10: update the memory
Compare the new position with the memorized position. Update the crow's memory with the new one if the crow's new position fitness is better than the crow's memorized position fitness. Otherwise, it will not change its memory. The updating memory is as following expression:

$$m_i^{t+1} = \begin{cases} X_i^{t+1} & \text{if } f(X_i^{t+1}) \geq f(m_i^t) \\ m_i^t & \text{Otherwise} \end{cases} \quad (16)$$

where f(.) is the fitness value.

Step 11: Check the termination criterion
Repeat steps 7 to 10 until reaching the tmax. After meeting the termination criterion, the optimal solution (best position) that achieves the minimum function for the optimization problem is saved. The distribution's new configuration, the sizes and placements of the DG, the fitness, VSI, Ploss, and Qloss values, active and reactive energy loss values, and the min and max bus voltages are all displayed in the optimal solution. The flow chart of the proposed methodology (simultaneous DNR and DG_SL during real-time operation mode) using CSA has been depicted in Fig. 2.

4 Simulation Result and Discussion

A comparative analysis using several DNs is used to evaluate the suggested methodology. MATLAB program simulates on a PC with a 3.07GHz CPU and 8GB RAM. Fig. 3 displays the load demand for 24 hours in p.u. [49]. The solar PV output generation according to sun radiation was taken in 2008 from the Kuantan location by the Malaysian Meteorological Department. Fig. 4 displays the PV generation output for a given day [50]. The results obtained are compared with the initial configuration (base case) to demonstrate the effectiveness of the suggested approach. As noted previously, the suggested method uses the CSA methodology in conjunction with the AHP approach to find the simultaneous optimal DNR integrated with optimal DG's-SL during real-time operating mode. The impact of the suggested approach was assessed on the optimization performance, VF, and energy loss to verify its influence.

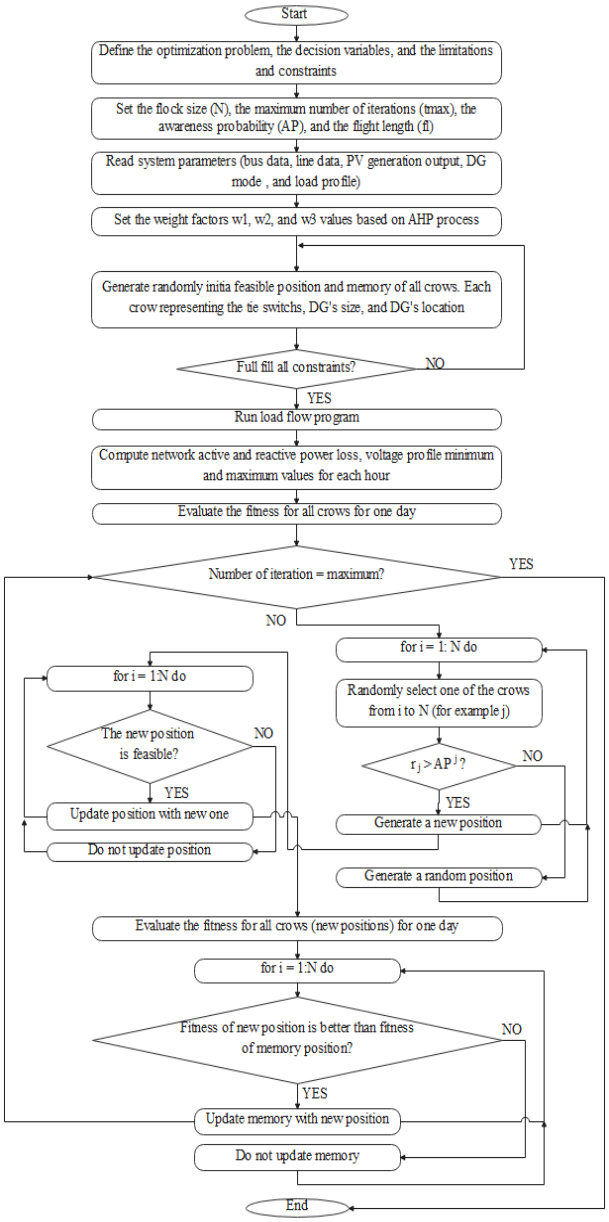

Fig. 2 Flow Chart of the simultaneous DNR and DG_SL during real-time operation mode using CSA.

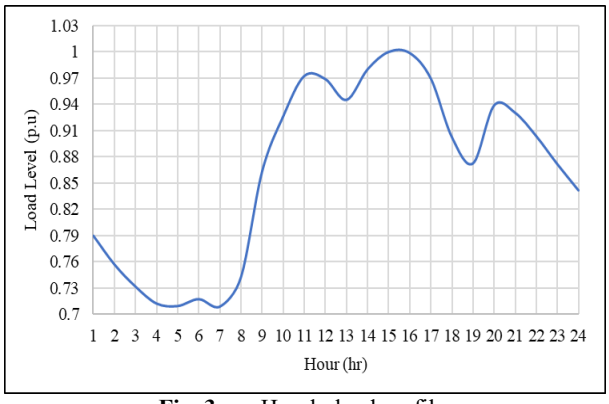

Fig. 3 Hourly load profile.

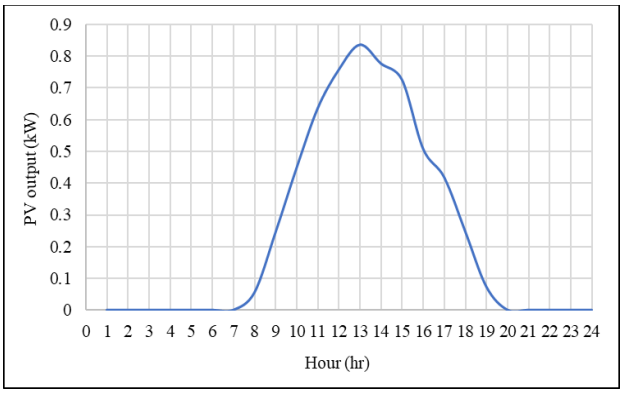

Fig. 4 Hourly PV power production.

Fig. 5 displays 33-bus test networks. Fig. 6 displays the 69-bus test network. The base voltage and apparent power of both networks are 12.66 kV and 100 MVA, respectively. In the 33-bus distribution, the five tie switches are 33, 34, 35, 36, and 37. The 69-bus distribution system configuration has five tie switches with the numbers 69, 70, 71, 72, and 73. The system's initial data for the 33-bus distribution is shown in Table 3's mid-column. The system's initial data for the 69-bus distribution is shown in Table 4's mid-column. More detailed information, such as buses' power load, and the line's resistance and reactance are reported in [51, 52] for both systems.

4.1 Impact of the Proposed Approach on the Power Loss

The primary goal of the suggested strategy is to minimize daily energy loss which reduces the overall amount of power drawn from the main source and increases system efficiency. Table 3 shows the obtained results of the 33-bus system compared to the initial case. The mid-column represents the initial case. The final column represents the simultaneous DNR integrated with optimal DG's-SL during real-time operation mode. The first compared item is the tie switch (normal open switch). From the results, the tie switches of the initial case are 33, 34, 35, 36, and 37. The optimal solution of the proposed approach changed the tie switches to 11, 33, 8, 25, and 32. The next compared item is Pl which is to be minimized. The system's apparent power load demand for one day (24 hours) for the initial case is (77,105.58+j 47,736.97) kVA. The active Pl is 287.314789 kW @ hr=15 and the reactive Pl is 213.443194 kWh @ hr=15. According to the proposed approach, the active Pl reduces to 19.890036 kW @ hr=15 and the reactive Pl reduces to 17.512196 kWh @ hr=15. The next compared item is total daily active and reactive energy loss which is to be minimized. For the initial case, the total daily active energy loss is 5106.974 kW and the total daily reactive energy loss is 3794.078 kWh. According to the proposed approach, the total daily active energy loss is reduced to 420.852086 kW

and the total daily reactive energy loss is reduced to 352.563858 kWh. Thus, the total daily active energy loss reduction is 91.7593% and the total daily reactive energy loss reduction is 90.7075%. The computational time taken for 300 iterations and 100 populations was 11665.46875s this time is suitable for solving complicated problems using CSA.

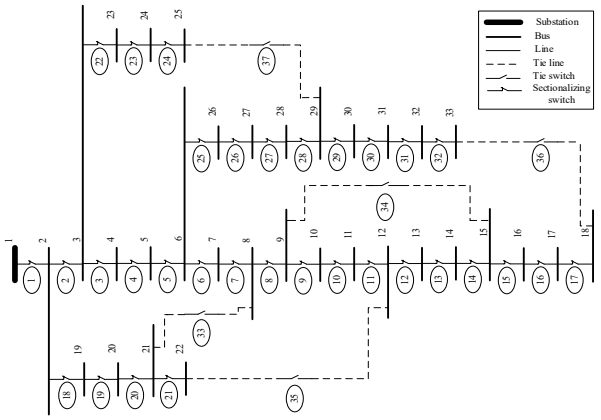

Fig. 5 The 33-bus radial system.

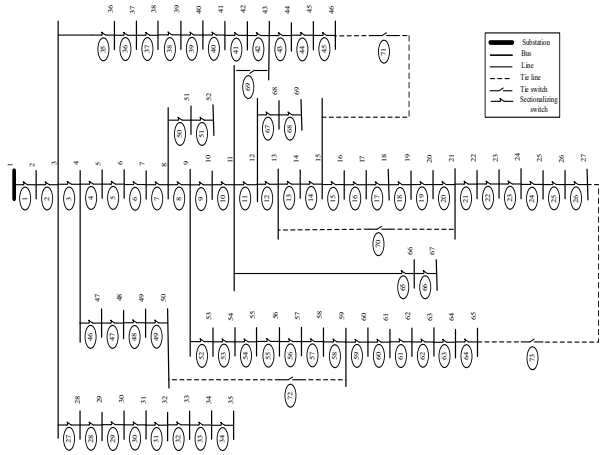

Fig. 6 The 69-bus radial system.

Table 4 shows the obtained results of the 69-bus system compared to the initial case. From the results, the tie switches of the initial case are 69, 70, 71, 72, and 73. The optimal solution of the proposed approach changed the tie switches to 62, 55, 20, 10, and 13. The next compared item is Pl which is to be minimized. The system's apparent power load demand for one day (24 hours) for the initial case is (78,908.9973+j 55,916.591395) kVA. The active Pl is 224.557257 kW @ hr=15 and the reactive Pl is 102.013498 kWh @ hr=15. According to the proposed approach, the active Pl reduces to 38.878 kW @ hr=15 and the reactive Pl reduces to 40.537 kWh @ hr=15. The next compared item is total daily active and reactive energy loss which is to be minimized. For the initial case, the total daily active energy loss is 4007.293 kW and the total daily reactive energy loss is 1822.504 kWh. According to the proposed approach, the total daily active energy loss is reduced to 729.823 kW and the total daily reactive energy loss is reduced to 732.923 kWh. Thus, the total daily active energy loss reduction is 81.7876% and the total daily reactive energy loss reduction is 59.7848%. The computational time taken for 300 iterations and 100 populations was 19730.78s this time is suitable for solving complicated problems using CSA. Based on a comparative analysis of the results, it can be concluded that the suggested method might yield the best results for simultaneous DNR integrated with optimal DG's-SL in real-time operating mode, hence maximizing the performance of both networks.

Table 3. A comparison of the 33-bus system's obtained findings.

Compared Item	Initial Form	Proposed approach using CSA
Tie Switch	33, 34, 35, 36, 37	11, 33, 8, 25, 32
Fitness	-------	2.75038449
Load Active Power P (kW)	77105.5778	77105.5778
Load Reactive Power Q (kVAR)	47736.96604	47736.96604
Active Pl (kW) @ hr=15	287.314789	19.890036
Reactive Pl (kVAR) @ hr=15	213.443194	17.512196
Total daily active Ples (kWh)	5106.974	420.852086
Total daily reactive Ples (kVARh)	3794.078	352.563858
Total daily active Pl reduction (%)	-------	91.7593
Total daily reactive Pl reduction (%)	-------	90.7075
CPU time(s)	-------	11665.46875

In this work, the DGs are considered to be biomass, photovoltaic (PV), and mini-hydro. Each DG has a maximum capacity of 2 MW. The mini-hydro and biomass DGs are operate in PQ mode, which generates constant active and reactive power. The photovoltaic unit operates in PV mode (i.e., the DG generates a certain active power and bus voltage). The DGs supply the optimized active power into the grid, and no reactive power is fed into the grid. This DG model is based on [53]. The bus voltage in this work is fixed at 1 p.u. Table 5 presents the obtained results of the DGs related to the proposed approach for the 33-bus system. The first DG sits as a biomass DG working under PQ mode and is located on bus 29 with 1.429585 kW output generation. The second DG sits as a photovoltaic DG working under PV mode and is located on bus 7. The output generation

of DG 2 is related to solar radiation shown in Fig. 4. The third DG sits as a mini-hydro DG working under PQ mode and is located on bus 15 with 0.718106826 kW output generation. Table 6 presents the obtained results of the DGs related to the proposed approach for the 69-bus system. The first DG sits as a biomass DG working under PQ mode and is located on bus 26 with 0.528375 kW output generation. The second DG sits as a photovoltaic DG working under PV mode and is located on bus 7. The output generation of DG 2 is related to solar radiation shown in Fig. 4. The third DG sits as a mini-hydro DG working under PQ mode and is located on bus 61 with 1.296753 kW output generation.

Table 4. A comparison of the 69-bus system's obtained findings.

Compared Item	Initial Form	Proposed approach using CSA
Tie Switch	69, 70, 71, 72, 73	62, 55, 20, 10, 13
Fitness	-------	7.142109
Load Active Power P (kW)	78908.9973	78908.9973
Load Reactive Power Q (kVAR)	55916.591395	55916.591395
Active Pl (kW) @ hr=15	224.557257	38.878
Reactive Pl (kVAR) @ hr=15	102.013498	40.537
Total daily active Ples (kWh)	4007.293	729.823
Total daily reactive Ples (kVARh)	1822.504	732.923
Total daily active Pl reduction (%)	-------	81.7876
Total daily reactive Pl reduction (%)	-------	59.7848
CPU time(s)	-------	19730.78

Table 5. DG operation mode for the 33-bus system.

DG NO	DG class	Mode	Location	Size
DG 1	biomass	PQ	29	1.429585
DG 2	photovoltaic	PV	7	PV generation
DG 3	mini-hydro	PQ	15	0.718106826

Table 6. DG operation mode of the 69-bus system.

DG NO	DG class	Mode	Location	Size
DG 1	biomass	PQ	26	0.528375
DG 2	photovoltaic	PV	42	PV generation
DG 3	mini-hydro	PQ	61	1.296753

Furthermore, the suggested method is predicated on identifying an optimal configuration that works for the full 24 hours of the day. To address implementation concerns and stop repeated on/off cycles from damaging switches (circuit breakers), one reconfiguration per day is required. As illustrated in Fig. 7, the ideal configuration (11, 33, 8, 25, and 32) for the 33-bus system is utilized to assess the daily active Pl. The daily active Pl is calculated using the 69-bus system's optimal configuration, which is represented in Fig. 8 (62, 55, 20, 10, and 13). The active Pl per hour using the suggested approach is significantly lower than the loss before reconfiguration, as can be seen in both figures.

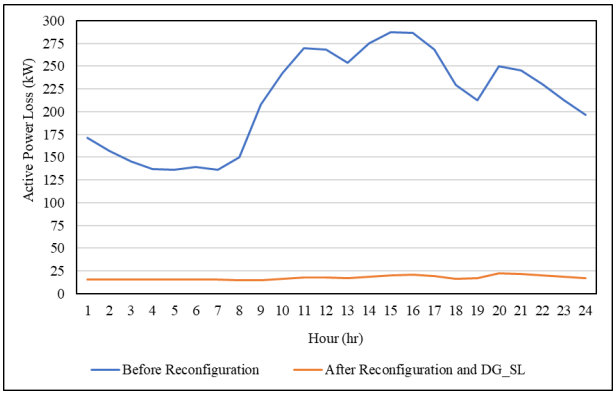

Fig. 7 Active Ples per hour for the 33-bus system.

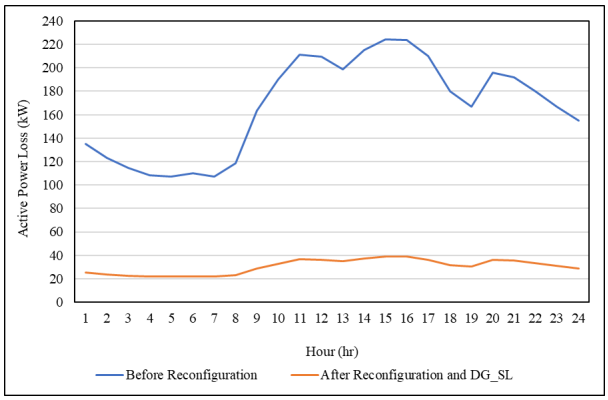

Fig. 8 Active Ples per hour for the 69-bus system.

Moreover, the daily reactive Pl for the 33-bus system is displayed in Fig. 9. The daily reactive Pl for the 69-bus system is displayed in Fig. 10. For both networks, the reactive Pl throughout each hour following the suggested method is significantly lower than the loss before reconfiguration.

4.2 Influence of the Proposed Approach on the Voltage Profile

Enhancing the VF makes the DDN more reliable and stable. Figs. 11 and 12 show, respectively, the network's lowest voltage values of the VF (p.u.) through 24 hours for the 33-bus and 69-bus systems. Both networks' min voltage bus values throughout 24 hours are consistently far better than their initial case (the min voltage bus values are almost equal to one power unit). In other words, the VF will be better than it was in the initial case

when using DG units in the DNR process during real-time operation mode.

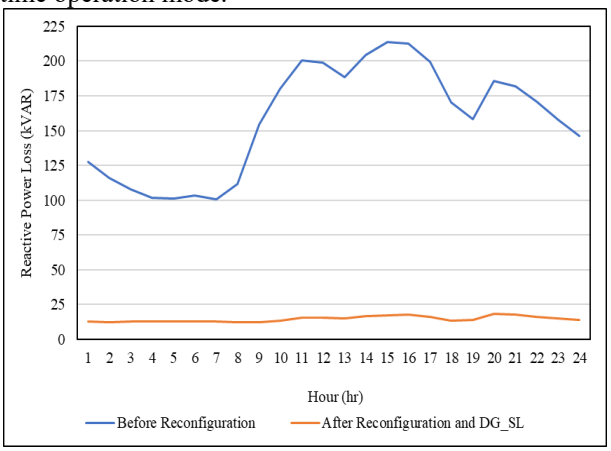

Fig. 9 Reactive Ples per hour for the 33-bus system.

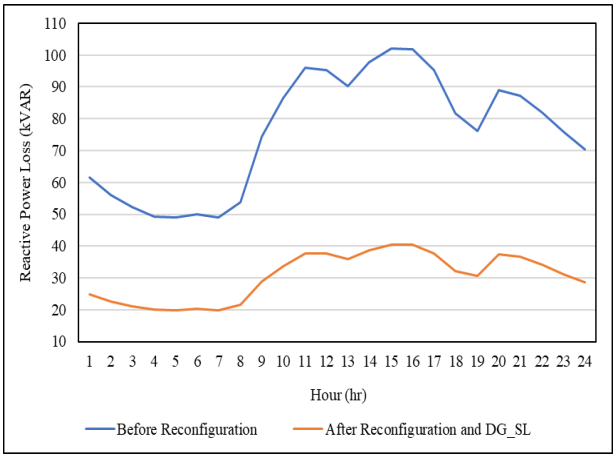

Fig. 10 Reactive Ples per hour for the 69-bus system.

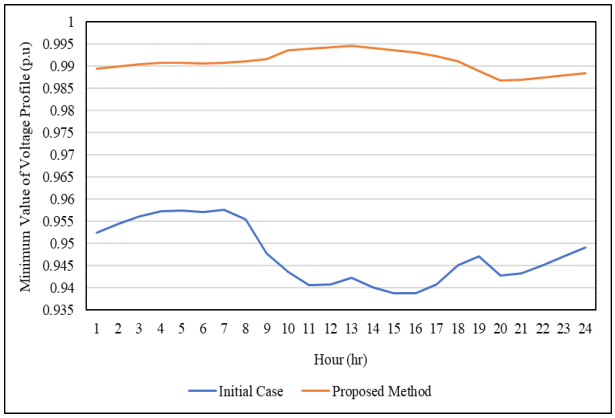

Fig. 11 Daily min values of the VF (p.u) for the 33-bus system.

4.3 Optimization Technique Performance Analysis for the Proposed Approach

Through the use of comparison, convergence, and robustness tests, the overall performance was assessed. The CSA's robustness was examined following 20 iterations of code execution. For the 33-bus system, the robustness curve is shown in Fig. 13. For the 69-bus system, Fig. 14 shows the robustness curve of the network. With all values for both figures being somewhat near to one another, the suggested CSA approach is extremely robust. This indicates that the system is more stable when the suggested way of simultaneous DNR integrated with DG units during real-time operating mode is used.

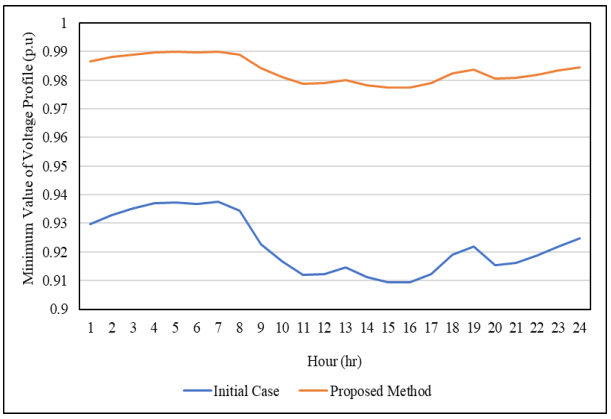

Fig. 12 Daily min values of the VF (p.u) for the 69-bus system.

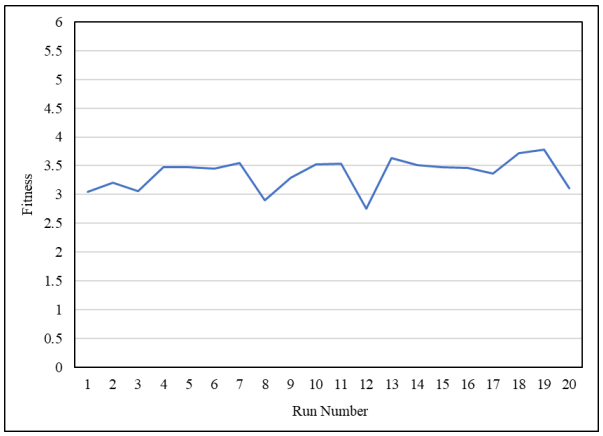

Fig. 13 The suggested method's robustness curves for the 33-bus system.

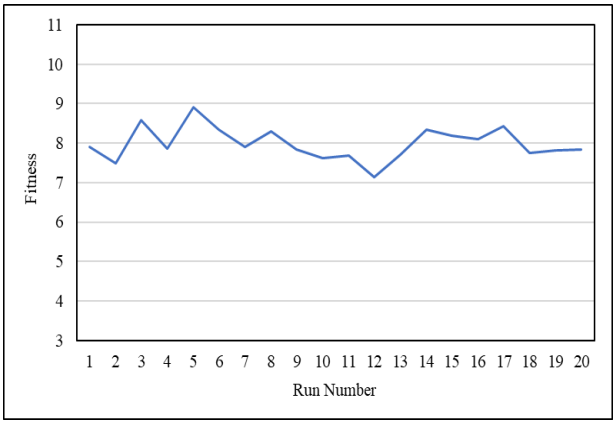

Fig. 14 The suggested method's robustness curves for the 69-bus system.

A statistical analysis of the CSA robustness test was also assessed. Tables 7 and 8 display the standard deviation (Std) for the IEEE-33 and IEEE-69 bus networks, respectively. It computes the lowest, max, and average values. Tables 7 and 8 show that a standard deviation close to zero is necessary for greater robustness. This suggests that the CSA was powerful and effective in determining the best solutions to a difficult problem.

Table 7. Statistical analysis of the 33-bus system.

Min value (Best)	Max value (Worst)	Av value (Mean)	Std
2.7503844	3.785722315	3.36687526	0.2664419

Table 8. Statistical analysis of the 69-bus system.

Min value (Best)	Max value (Worst)	Av value (Mean)	Std
7.142109	8.908563	7.9879	0.401503

The CSA convergence toward the global optimal solution was further assessed for validation. After 20 independent runs of the simulation, 20 local optima were obtained, and the best among them was identified as the global optimum. In Figs. 15 and 16, the convergence of the global optimum is highlighted in green (run number 12) against the other runs for the 33-bus and 69-bus systems, respectively. The convergence curves demonstrate that the CSA continues to evolve throughout all 300 iterations, indicating that, unlike conventional algorithms, the proposed CSA approach is not confined to local optima.

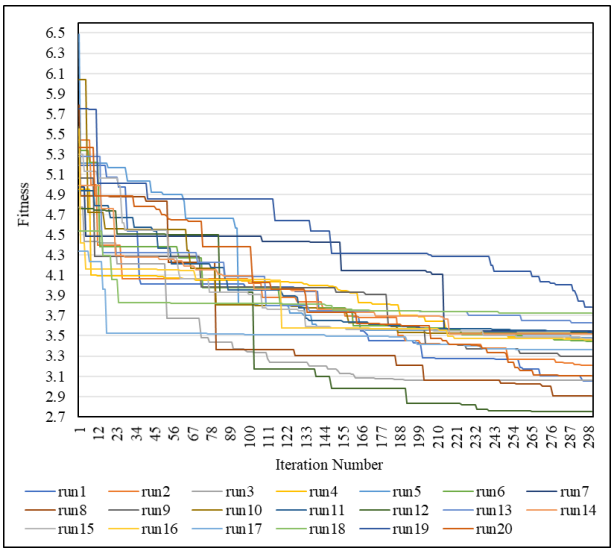

Fig. 15 Convergence curves for the 33-bus system using the suggested approach.

Additionally, a comparison was made between the effectiveness of the Static Distribution Reconfiguration (DR) and DG_SL approach with that of previously published studies. The comparison results for the 33-bus system are shown in Table 9. In comparison with alternative algorithms, the CSA technique leads to a 51.846 kW Pl. The decreased loss so reaches its max value of 74.41%. The comparison results for the 69-bus system are shown in Table 10. In comparison with alternative algorithms, the CSA technique leads to a 37.982 kW Pl. Consequently, the biggest reduction loss (83.086%) is experienced. The recommended CSA method produces the best outcomes when compared to other approaches. Consequently, the best results were obtained when CSA was used to perform simultaneous DNR with DG_SL.

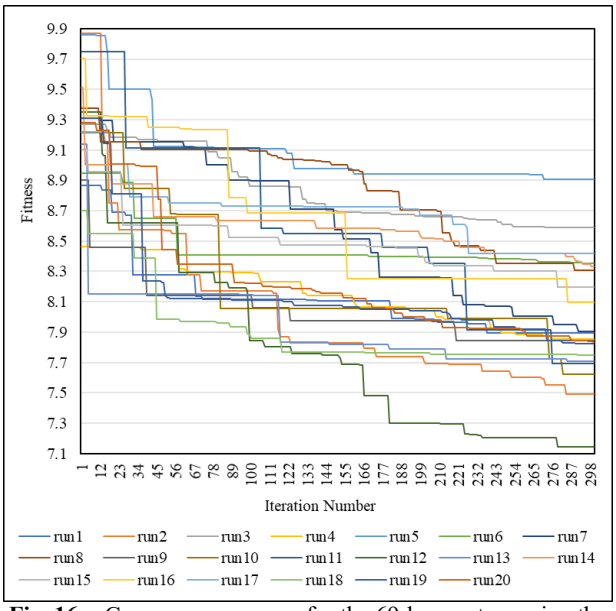

Fig. 16 Convergence curves for the 69-bus system using the suggested approach.

Table 9. Comparison results of several algorithms of the 33-bus system.

Methods	Tie Switch	Min bus's Voltage (pu)	Ploss (kW)	Loss Reduction (%)
HSA [54]	7, 28, 10, 32, 14	0.97	73.1	63.9
FWA [55]	7, 32, 11, 14, 28	0.97	67.1	66.9
EP [56]	7, 32, 8, 9, 28,	0.97	73.97	63.5
PSO [56]	7, 13, 28, 32, 10	0.97380	72.4210	64.3
GSA [56]	7, 13, 28, 32, 9	0.97420	72.4250	64.250

FA [56]	7, 13, 28, 32, 10	0.975	72.3610	64.280
PSO [57]	7, 14, 28, 32, 9	0.96110	64.910	67.960
MPSO [58]	7,14, 32, 37, 9	0.97640	62.40	68.320
ISCA [59]	7, 14, 28. 31, 9	-	66.810	67.030
FA [60]	7, 14, 27, 30, 35	0.975	57.637	71.55
FA [61]	34, 28, 11, 32, 33	0.969724	54.997	72.83
The Proposed Method by CSA	**34, 11, 31, 28, 33**	**0.977619**	**51.846**	**74.41**

Table 10. Comparison results of several algorithms of the 69-bus system.

Methods	Tie (Open) Switch	Min bus's Voltage (pu)	Ploss (kW)	Loss Reduction (%)
GA [54]	10, 62, 15, 45, 55	0.973	46.5	73.4
RGA [54]	10, 62, 16, 14, 55	0.974	44.230	80.3
HSA [54]	69, 61, 17, 13, 58	0.974	40.3	82.1
FWA [55]	69, 55, 63, 70, 13	0.980	39.25	82.6
MPSO [58]	14, 69, 70, 58-61	0.9899	42.2	81.10
ISCA [59]	12, 63, 69, 9, 57	-	39.73	82.33
FA [61]	13, 12, 62, 10, 57	0.98035	39.16	82.6
The Proposed Method by CSA	**10, 58, 17, 13, 63**	**0.981438**	**37.982**	**83.086**

5 Conclusion

This research proposes a novel, simultaneous approach to enhance the stability and reliability of the dynamic distribution network (DDN) in real-time operation mode by using DNR with DG_SL. This technique offers the possibility to reduce the DDN's active and reactive total daily energy losses while enhancing the Voltage Stability Index, increasing network efficiency, and balancing load. To accomplish these objectives, the AHP in conjunction with the CSA constituted the basis of the MODMA. The AHP approach is used to calculate the fitness weight factors, and the meta-heuristic technique based on the CSA is used to calculate the minimum fitness. The efficacy of the proposed method is verified with 33-bus and 69-bus DDNs. The encouraging results show that the proposed method is very effective and efficient at finding the global optimal solution of the DNR and optimal DG_SL while staying within the bounds set by the network power flow, voltage limitations, output generation of renewable energy resources, distributed generation mode, and network load profile. The proposed AHP–CSA framework achieved up to 91.75% reduction in daily active losses and more than 90% reduction in daily reactive losses for the IEEE 33-bus system, and up to 81.78% and 59.78% reductions, respectively, for the IEEE 69-bus system. In both cases, the Voltage Stability Index was consistently improved toward unity, confirming the robustness and reliability of the approach for real-time distribution network operation with renewable DG integration. The results confirm that the proposed methodology could support Real-Time Operation systems with Renewable Energy Distributed generator units and potentially increase network stability and reliability. Moreover, the results show how well CSA performs in identifying the global optimal solution to complex problems, such as the DG_SL and DNR difficulties that increase system performance in operation mode. Part of the results were also contrasted with those from other published articles, showcasing the effectiveness of the CSA in comparison to outcomes derived from the application of metaheuristic approaches.

Conflict of Interest

The author declares no conflict of interest.

Author Contributions

This work was done by the sole author, Ola Badran.

Funding

No funding was received for this work.

Informed Consent Statement

Not applicable.

Acknowledgment

The authors would like to thank Palestine Technical University-Kadoorie for supporting them financially.

References

[1] O. Badran, S. Mekhilef, H. Mokhlis, and W. Dahalan, "Optimal reconfiguration of distribution system connected with distributed generations: A review of different methodologies," *Renewable and Sustainable Energy Reviews,* vol. 73, pp. 854-867, 2017.

[2] F. E. Riaño, J. F. Cruz, O. D. Montoya, H. R. Chamorro, and L. Alvarado-Barrios, "Reduction of losses and operating costs in distribution networks using a genetic algorithm and mathematical optimization," *Electronics,* vol. 10, no. 4, p. 419, 2021.

[3] O. D. Montoya, A. Molina-Cabrera, H. R. Chamorro, L. Alvarado-Barrios, and E. Rivas-Trujillo, "A Hybrid approach based on SOCP and the discrete version of the SCA for optimal placement and sizing DGs in AC distribution networks," *Electronics,* vol. 10, no. 1, p. 26, 2020.

[4] O. S. Bdran, "Distribution Network Performance Enhancement Using Reconfiguration Technique based on Gravitational Search Algorithm," *Palestinian Journal of Technology and Applied Sciences (PJTAS),* vol. 1, no. 8, Articles, 06/02 2025, doi: 10.33977/2106-000-008-001.

[5] M. R. Andervazh, J. Olamaei, and M. R. Haghifam, "Adaptive multi-objective distribution network reconfiguration using multi-objective discrete particles swarm optimisation algorithm and graph theory," *IET Generation, Transmission & Distribution,* vol. 7, no. 12, pp. 1367-1382, 2013.

[6] R. Taleski and D. Rajicic, "Distribution network reconfiguration for energy loss reduction," *IEEE Transactions on Power systems,* vol. 12, no. 1, pp. 398-406, 1997.

[7] L.-L. Li, X.-D. Fan, K.-J. Wu, K. Sethanan, and M.-L. Tseng, "Multi-objective distributed generation hierarchical optimal planning in distribution network: Improved beluga whale optimization algorithm," *Expert Systems with Applications,* vol. 237, p. 121406, 2024.

[8] O. Badran, "IEEE-69 Distribution Network Performance Improvement by Simultaneously Optimal Distributed Generation Sizing and Location Using PSO Algorithm," *Palestine Technical University Kadoorie, Tulkarm, Palestine,* vol. 11, no. 1, pp. 01-15, 2023, doi: https://doi.org/10.53671/pturj.v11i1.313.

[9] N. S. Rau and Y.-h. Wan, "Optimum location of resources in distributed planning," *IEEE Transactions on Power systems,* vol. 9, no. 4, pp. 2014-2020, 1994.

[10] L. A. Wong, V. K. Ramachandaramurthy, P. Taylor, J. Ekanayake, S. L. Walker, and S. Padmanaban, "Review on the optimal placement, sizing and control of an energy storage system in the distribution network," *Journal of Energy Storage,* vol. 21, pp. 489-504, 2019.

[11] M. P. HA, P. D. Huy, and V. K. Ramachandaramurthy, "A review of the optimal allocation of distributed generation: Objectives, constraints, methods, and algorithms," *Renewable and Sustainable Energy Reviews,* vol. 75, pp. 293-312, 2017.

[12] A. J. G. Mena and J. A. M. García, "An efficient approach for the siting and sizing problem of distributed generation," *International Journal of Electrical Power & Energy Systems,* vol. 69, pp. 167-172, 2015.

[13] H. S. Avchat and S. Mhetre, "Optimal placement of distributed generation in distribution network using particle swarm optimization," in *2020 International Conference for Emerging Technology (INCET)*, 2020: IEEE, pp. 1-5.

[14] E. Karunarathne, J. Pasupuleti, J. Ekanayake, and D. Almeida, "The optimal placement and sizing of distributed generation in an active distribution network with several soft open points," *Energies,* vol. 14, no. 4, p. 1084, 2021.

[15] O. Al-Qasem and J. Jallad, "Experimental Characterization of Lead–Acid Storage Batteries used in PV Power Systems," *International Journal of Advanced Research in Electrical, Electronics and Instrumentation Engineering,* vol. 3, no. 4, 2014.

[16] O. S. W. Al-Qasem, "Modeling and simulation of lead-acid storage batteries within photovoltaic power systems," *A Thesis Presented to the An-Najah National University, Palestine,* 2012.

[17] L. H. Macedo, J. F. Franco, M. Mahdavi, and R. Romero, "A contribution to the optimization of the reconfiguration problem in radial distribution systems," *Journal of Control, Automation and Electrical Systems,* vol. 29, no. 6, pp. 756-768, 2018.

[18] H. Hosseini, S. Jalilzadeh, V. Nabaei, G. Z. Govar, and M. Mahdavi, "Enhancing deregulated distribution network reliability for minimizing penalty cost based on reconfiguration using BPSO," in *2008 IEEE 2nd International Power and Energy Conference*, 2008: IEEE, pp. 983-987.

[19] W. Zheng, W. Huang, D. J. Hill, and Y. Hou, "An adaptive distributionally robust model for three-phase distribution network reconfiguration," *IEEE Transactions on Smart Grid,* vol. 12, no. 2, pp. 1224-1237, 2020.

[20] M. Mahdavi, H. H. Alhelou, N. D. Hatziargyriou, and A. Al-Hinai, "An efficient mathematical model for distribution system reconfiguration using

AMPL," *IEEE Access,* vol. 9, pp. 79961-79993, 2021.
[21] A. Uniyal and S. Sarangi, "Optimal network reconfiguration and DG allocation using adaptive modified whale optimization algorithm considering probabilistic load flow," *Electric Power Systems Research,* vol. 192, p. 106909, 2021.
[22] Q. Shi *et al.*, "Network reconfiguration and distributed energy resource scheduling for improved distribution system resilience," *International Journal of Electrical Power & Energy Systems,* vol. 124, p. 106355, 2021.
[23] A. M. Shaheen, A. M. Elsayed, R. A. El-Sehiemy, and A. Y. Abdelaziz, "Equilibrium optimization algorithm for network reconfiguration and distributed generation allocation in power systems," *Applied Soft Computing,* vol. 98, p. 106867, 2021.
[24] T. T. Nguyen, T. T. Nguyen, L. T. Duong, and V. A. Truong, "An effective method to solve the problem of electric distribution network reconfiguration considering distributed generations for energy loss reduction," *Neural Computing and Applications,* vol. 33, pp. 1625-1641, 2021.
[25] O. Bdran, "Loss Minimization and Voltage Enhancement Through DGs Generation and Sittings Considering TCA in Network Reconfiguration during Load-Variation," *Palestine Technical University Research Journal,* vol. 12, no. 3, 12/30 2024, doi: 10.53671/pturj.v12i3.562.
[26] O. Badran and J. Jallad, "Active and Reactive Power loss Minimization Along with Voltage profile Improvement for Distribution Reconfiguration," *International Journal of Electrical and Computer Engineering Systems,* vol. 14, no. 10, pp. 1193-1202, 12/06 2023, doi: 10.32985/ijeces.14.10.12.
[27] M. R. Islam, H. Lu, M. Hossain, and L. Li, "Mitigating unbalance using distributed network reconfiguration techniques in distributed power generation grids with services for electric vehicles: A review," *Journal of Cleaner Production,* vol. 239, p. 117932, 2019.
[28] I. B. Hamida, S. B. Salah, F. Msahli, and M. F. Mimouni, "Optimal network reconfiguration and renewable DG integration considering time sequence variation in load and DGs," *Renewable energy,* vol. 121, pp. 66-80, 2018.
[29] S. Essallah and A. Khedher, "Optimization of distribution system operation by network reconfiguration and DG integration using MPSO algorithm," *Renewable Energy Focus,* vol. 34, pp. 37-46, 2020.
[30] M. F. Abd El-salam, E. Beshr, and M. B. Eteiba, "A new hybrid technique for minimizing power losses in a distribution system by optimal sizing and siting of distributed generators with network reconfiguration," *Energies,* vol. 11, no. 12, p. 3351, 2018.
[31] M. N. A. Rahim, H. Mokhlis, A. H. A. Bakar, M. T. Rahman, O. Badran, and N. N. Mansor, "Protection coordination toward optimal network reconfiguration and DG sizing," *IEEE Access,* vol. 7, pp. 163700-163718, 2019.
[32] R. Fathi, B. Tousi, and S. Galvani, "Allocation of renewable resources with radial distribution network reconfiguration using improved salp swarm algorithm," *Applied Soft Computing,* vol. 132, p. 109828, 2023.
[33] D. Swaminathan and A. Rajagopalan, "Optimized network reconfiguration with integrated generation using tangent golden flower algorithm," *Energies,* vol. 15, no. 21, p. 8158, 2022.
[34] O. Badran, J. Jallad, H. Mokhlis, and S. Mekhilef, "Network reconfiguration and DG output including real time optimal switching sequence for system improvement," *Australian Journal of Electrical and Electronics Engineering,* vol. 17, no. 3, pp. 157-172, 2020.
[35] O. Badran, H. Mokhlis, S. Mekhilef, W. Dahalan, and J. Jallad, "Minimum switching losses for solving distribution NR problem with distributed generation," *IET Generation, Transmission & Distribution,* vol. 12, no. 8, pp. 1790-1801, 2018.
[36] O. Badran, S. Mekhilef, H. Mokhlis, and W. Dahalan, "Optimal switching sequence path for distribution network reconfiguration considering different types of distributed generation," *IEEJ Transactions on Electrical and Electronic Engineering,* vol. 12, no. 6, pp. 874-882, 2017.
[37] S. F. Santos, M. Gough, D. Z. Fitiwi, J. Pogeira, M. Shafie-khah, and J. P. Catalão, "Dynamic distribution system reconfiguration considering distributed renewable energy sources and energy storage systems," *IEEE Systems Journal,* vol. 16, no. 3, pp. 3723-3733, 2022.
[38] M. R. Dorostkar-Ghamsari, M. Fotuhi-Firuzabad, M. Lehtonen, and A. Safdarian, "Value of distribution network reconfiguration in presence of renewable energy resources," *IEEE Transactions on Power systems,* vol. 31, no. 3, pp. 1879-1888, 2015.
[39] H. Zhan, C. Jiang, and J. Lin, "A novel dynamic reconfiguration approach for active distribution networks with soft open points and energy storage systems," *Energy Reports,* vol. 13, pp. 1875-1887, 2025.
[40] O. B. Kundačina, P. M. Vidović, and M. R. Petković, "Solving dynamic distribution network reconfiguration using deep reinforcement learning," *Electrical Engineering,* vol. 104, no. 3, pp. 1487-1501, 2022.
[41] M. Chakravorty and D. Das, "Voltage stability analysis of radial distribution networks,"

International Journal of Electrical Power & Energy Systems, vol. 23, no. 2, pp. 129-135, 2001.

[42] J. Shukla, B. Das, and V. Pant, "Consideration of small signal stability in multi-objective DS reconfiguration in the presence of distributed generation," *IET Generation, Transmission & Distribution,* vol. 11, no. 1, pp. 236-245, 2017.

[43] T. Fetouh and A. M. Elsayed, "Optimal control and operation of fully automated distribution networks using improved tunicate swarm intelligent algorithm," *IEEE Access,* vol. 8, pp. 129689-129708, 2020.

[44] H. Xing and S. Hong, "Ordinal optimisation approach for complex distribution network reconfiguration," *The Journal of Engineering,* vol. 2019, no. 18, pp. 5055-5058, 2019.

[45] A. Askarzadeh, "A novel metaheuristic method for solving constrained engineering optimization problems: crow search algorithm," *Computers & structures,* vol. 169, pp. 1-12, 2016.

[46] S. R. Salkuti, "Multi-objective based optimal network reconfiguration using crow search algorithm," *International Journal of Advanced Computer Science and Applications,* vol. 12, no. 3, 2021.

[47] C. Vasavi and T. G. Manohar, "OPTIMAL PLACEMENT OF DG AND TCI-FCL SIZING USING CROW SEARCH ALGORITHM," *International Journal of Electrical Engineering and Technology (IJEET),* vol. 11, no. 5, pp. 43-54, July 2020.

[48] A. K. Pandey and S. Kirmani, "Multi-objective optimal location and sizing of hybrid photovoltaic system in distribution systems using crow search algorithm," *International Journal of Renewable Energy Research,* vol. 9, no. 4, pp. 1681-1693, 2019.

[49] K. G. Ing, H. Mokhlis, H. A. Illias, M. M. Aman, and J. J. Jamian, "Gravitational search algorithm and selection approach for optimal distribution network configuration based on daily photovoltaic and loading variation," *Journal of Applied Mathematics,* vol. 2015, no. 1, p. 894758, 2015.

[50] N. H. B. JALAN, "Operating Code 1: Demand Forecast, The Malaysia Grid Code Awareness Programme," *Kuala Lupur.,* 2014.

[51] M. E. Baran and F. F. Wu, "Network reconfiguration in distribution systems for loss reduction and load balancing," *IEEE Transactions on Power delivery,* vol. 4, no. 2, pp. 1401-1407, 1989.

[52] Y. Latreche, H. Bouchekara, K. Naidu, H. Mokhlis, and W. Dahalan, "Comprehensive review of radial distribution test systems," *TechRxiv,* vol. 1, pp. 1-65, 2020.

[53] K. Gia Ing, J. J. Jamian, H. Mokhlis, and H. A. Illias, "Optimum distribution network operation considering distributed generation mode of operations and safety margin," *IET Renewable Power Generation,* vol. 10, no. 8, pp. 1049-1058, 2016.

[54] R. S. Rao, K. Ravindra, K. Satish, and S. Narasimham, "Power loss minimization in distribution system using network reconfiguration in the presence of distributed generation," *IEEE transactions on power systems,* vol. 28, no. 1, pp. 317-325, 2012.

[55] A. M. Imran, M. Kowsalya, and D. Kothari, "A novel integration technique for optimal network reconfiguration and distributed generation placement in power distribution networks," *International Journal of Electrical Power & Energy Systems,* vol. 63, pp. 461-472, 2014.

[56] O. Badran, H. Mokhlis, S. Mekhilef, and W. Dahalan, "Multi-Objective network reconfiguration with optimal DG output using meta-heuristic search algorithms," *Arabian Journal for Science and Engineering,* vol. 43, pp. 2673-2686, 2018.

[57] W. Haider, S. J. U. Hassan, A. Mehdi, A. Hussain, G. O. M. Adjayeng, and C.-H. Kim, "Voltage profile enhancement and loss minimization using optimal placement and sizing of distributed generation in reconfigured network," *Machines,* vol. 9, no. 1, p. 20, 2021.

[58] A. A. M. Zin, A. K. Ferdavani, A. B. Khairuddin, and M. M. Naeini, "Reconfiguration of radial electrical distribution network through minimum-current circular-updating-mechanism method," *IEEE transactions on power systems,* vol. 27, no. 2, pp. 968-974, 2011.

[59] U. Raut and S. Mishra, "An improved sine–cosine algorithm for simultaneous network reconfiguration and DG allocation in power distribution systems," *Applied Soft Computing,* vol. 92, p. 106293, 2020.

[60] O. Badran and J. Jallad, "Multi-objective decision approach integrated with Loadability and weight factor analysis for reconfiguration with DG sizing and allocation including tap changer," *Arabian Journal for Science and Engineering,* vol. 48, no. 5, pp. 6797-6818, 2023.

[61] O. Badran and J. Jallad, "Multi-Objective Decision Approach for Optimal Real-Time Switching Sequence of Network Reconfiguration Realizing Maximum Load Capacity," *Energies,* vol. 16, no. 19, p. 6779, 2023.

Biography

Ola Badran received the B.E. degree (Hons) in Electrical Engineering from Palestine Technical University-Kadoorie, Palestine, in 2008, and the M.E. degree (Hons) in clean energy engineering and conservation of consumption from An-Najah National University, Palestine, in 2012. Ph.D. degree in Electrical Engineering - Power System from the University of Malaya in 2018. Her research interests include network reconfiguration, DG sizing and location, optimization techniques, and renewable energy. She can be contacted at email: o.badran@ptuk.edu.ps.